Physica A 173 (1991) 332–362
North-Holland

THE THERMAL CONDUCTIVITY AND HEAT CAPACITY OF FLUID NITROGEN*

R.A. PERKINS, H.M. RODER and D.G. FRIEND
Thermophysics Division, National Institute of Standards and Technology, Boulder, CO 80303, USA

C.A. NIETO DE CASTRO[1]
Departamento de Quimica, Faculdade de Ciências, Universidade de Lisboa, R. Ernesto Vasconcelos, Bloco C1, 1700 Lisbon, Portugal

Received 29 June 1990
Revised manuscript received 23 November 1990

This paper presents new absolute measurements of the thermal conductivity and the thermal diffusivity of nitrogen made with a transient hot wire instrument. The instrument measures the thermal conductivity with an uncertainty less than ±1% and the thermal diffusivity with an uncertainty of ±5% except at the fluid critical point. The data cover the region from 80 to 300 K at pressures to 70 MPa. The data consist of 8 supercritical isotherms, 3 vapor isotherms, and 4 liquid isotherms.

A surface fit is developed for our nitrogen thermal conductivity data from 80 to 300 K at pressures to 70 MPa. The data are compared with a recent theory for the first density coefficient of thermal conductivity and a new mode-coupling theory for the thermal conductivity critical enhancement. These data illustrate that it is necessary to study a fluid over a wide range of temperatures and densities in order to characterize the thermal conductivity surface.

Isobaric heat capacity results were determined from the simultaneously measured values of thermal conductivity and thermal diffusivity, using the density calculated from an equation of state. The heat capacities obtained by this technique are compared to the heat capacities predicted by a recent equation of state developed specifically for nitrogen.

1. Introduction

Although the thermal conductivity of nitrogen has been widely studied, there are large regions of the phase diagram below 300 K where there are no data available. There are two low temperature experimental studies of nitrogen thermal conductivity which cover the region 70 to 200 K and 0 to 15 MPa [1, 2].

* Contribution of the National Institute of Standards and Technology, not subject to copyright.
[1] Also Centro de Quimica Estrutural, Complexo I, IST, 1096 Lisbon Codex, Portugal.

Recently Millat, Ross and Wakeham [3] reported results from 177 to 277 K at pressures to 10 MPa. No data are reported at pressures above 15 MPa at temperatures below 295 K. The thermal conductivity of nitrogen has been studied between 295 and 400 K by a number of researchers [4–15]. Tufeu et al. [10] report measurements of nitrogen thermal conductivity at 300 K to pressures of 1000 MPa.

In addition to the thermal conductivity, thermal diffusivity can be measured with transient hot wire instruments. These fluid thermal diffusivity measurements can be made with fair accuracy over wide ranges of density [16–18]. The isobaric heat capacity can be obtained from the measurements of thermal conductivity and thermal diffusivity, provided that the density is known.

We report extensive measurements of the thermal conductivity and thermal diffusivity of nitrogen in the range 80 to 300 K, at pressures up to 70 MPa. The measurements cover the vapor, compressed liquid, and supercritical dense gas states. The thermal conductivity data are compared to several correlations [19–21]. A surface fit of the thermal conductivity data as a function of temperature and density is also described. The thermal conductivity data have an uncertainty of less than ±1%, except for data near the fluid critical point, while the thermal diffusivity and heat capacity data have an estimated uncertainty of ±5%. The maximum uncertainty in the thermal conductivity is about ±3%, and in the thermal diffusivity it is about ±10%, for the 131 K isotherm near the critical density.

2. Experimental technique

The transient hot wire is now widely accepted as an accurate method for the measurement of the thermal conductivity of fluids [22]. Its working equation, including the applicable corrections, is well established. The working equation for the temperature rise of the fluid at the surface of the wire where $r = r_0$ at time t, is given by

$$\Delta T_{id}(r_0, t) = \frac{q}{4\pi\lambda} \ln\left(\frac{4at}{r_0^2 C}\right) = \frac{q}{4\pi\lambda} \ln\left(\frac{4a}{r_0^2 C}\right) + \frac{q}{4\pi\lambda} \ln(t) . \tag{1}$$

In eq. (1), q is the power input per unit length of wire, λ is the thermal conductivity, $a = \lambda/\rho C_p$ is the thermal diffusivity of the fluid, ρ is the density, C_p is the isobaric heat capacity, and $C = 1.781\ldots$ is the exponential of Euler's constant. We use eq. (1) and deduce the thermal conductivity from the slope of the straight line of ΔT_{id} versus $\ln(t)$.

The working equation for the thermal diffusivity is

$$a = \frac{r_0^2 C}{4t'} \exp\left(\frac{4\pi\lambda \, \Delta T_{id}(r_0, t')}{q} \right) . \tag{2}$$

The thermal diffusivity is obtained from λ and a value of ΔT_{id} at an arbitrary time t'; that is, $\Delta T_{id}(r_0, t')$ is the intercept of eq. (1) if t' is selected as 1 s. Sources of departure from the working equations have been investigated recently for both thermal conductivity and thermal diffusivity [16, 17].

The thermal conductivity is reported at the reference temperature T_r and density ρ_r defined in eq. (3) below. The thermal diffusivity calculated from eq. (2) must be referred to the conditions at zero time, that is, to the bath or cell temperature. In summary, the thermal conductivity and the thermal diffusivity evaluated by the data reduction program are related to the reference state variables and to the zero time cell variables as follows:

$$\begin{aligned} &\lambda = \lambda(T_r, \rho_r) , \qquad T_r = T_0 + 0.5[\Delta T(t_{\text{initial}}) + \Delta T(t_{\text{final}})] , \\ &\rho_r = \rho(T_r, P_0) , \qquad a = a(\rho_0, T_0) = \frac{\lambda(T_0, \rho_0)}{\rho_0 (C_p)_0} , \\ &\rho_0 = \rho(T_0, P_0) , \qquad (C_p)_0 = C_p(T_0, P_0) , \end{aligned} \tag{3}$$

where P_0 is the equilibrium pressure at time $t = 0$.

3. Apparatus

The apparatus used for the measurements is described in ref. [11]. The measurements are made with a 12.7 μm diameter platinum wire at times of up to 1 s. The hot wire and a shorter compensating hot wire are arranged in opposing arms of a Wheatstone bridge. The cell containing the core of the apparatus is designed to accommodate pressures from near 0 to 70 MPa and temperatures from 78 to 330 K. The data acquisition system is controlled by a microcomputer and includes two programmable digital voltmeters. We measure the temperature rise of the hot wire at 250 fixed times, 4 ms apart, with a modified Wheatstone bridge. We then use linear regression to arrive at the slope and intercept of the line through the temperature rise as a function of log time.

To obtain accurate results for the thermal diffusivity, and ultimately for the heat capacity, some changes were made in the original apparatus. These changes improve the measurement of resistance for both the bridge and the wires, improve the nulling of the bridge prior to application of power, improve the timing of the experiment, provide some redundancy in the measurement capability, and reduce the noise in the voltage measurements across the bridge.

In particular, since our first measurements of thermal diffusivity [16], a reversing switch driven by the computer was added to the system to improve the resistance measurements in the bridge arms and the zero offset, by eliminating any thermal e.m.f.'s present in the wire and lead connections.

The instrument performance has been fully tested during recent measurements on argon [18, 23, 24]. At 300.65 K the divergence of the results obtained at different applied powers, corresponding to different temperature rises, is less than 0.6%. The deviation of the corrected experimental temperature rise from the linear fit is better than 0.2%. Fig. 1 shows a scattering diagram for a nitrogen experiment at 130.03 K and 61.543 MPa; the deviations from the ideal model are less than 0.03%. Detailed comparisons were made between this instrument and a transient hot wire instrument at Lisbon, Portugal [25, 26] with liquid argon over three isotherms. The maximum deviation between the two instruments was found to be 1.3% with an average deviation of 0.5%. This agreement indicates that the thermal conductivity data have an uncertainty of less than $\pm 1\%$ in regions away from the critical point.

The nitrogen used for the measurements has a purity in excess of 99.999%. A small diaphragm compressor was used to pressurize the thermal conductivity cell during the experiments.

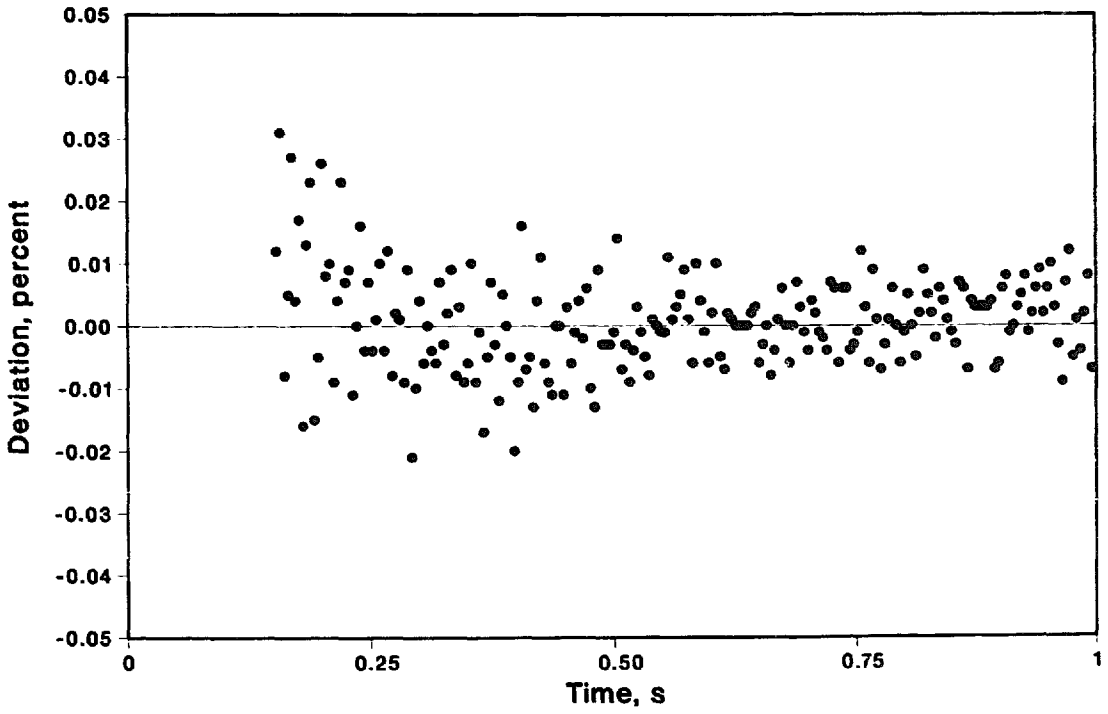

Fig. 1. Deviations from ideal temperature rise for nitrogen gas at 130.03 K and 61.543 MPa.

4. Results

A total of 1511 data points were measured along three vapor isotherms, four compressed liquid isotherms, and eight supercritical isotherms. For each pressure, four data points with different powers were taken to verify the absence of convection. These four points were subsequently averaged, and the averages are presented in tables I, II and III. The pressure, temperature and applied power were measured directly, while the density was calculated with the equation of state of Jacobsen et al. [27]. A complete tabulation of the data is given in ref. [24]. The results for the thermal conductivity were adjusted at constant density to the nominal isothermal temperature using the surface fit developed in this work. These adjustments were generally less than 0.2% except near the critical point. The thermal diffusivity and heat capacity results were also adjusted to the nominal temperature and density using the equation of state of Jacobsen et al. [27].

The error in the thermal conductivity depends on the thermodynamic state of the fluid. Along a normal isotherm, the error decreases from low to high

Table I
The thermal conductivity, thermal diffusivity, and heat capacity of nitrogen vapor.

Nominal temperature T_n (K)	Cell pressure P (MPa)	Nominal density $\rho_n(T_n, P)$ (mol ℓ^{-1})	Thermal conductivity $\lambda_n(T_n, \rho_n)$ (W m^{-1} K^{-1})	Thermal diffusivity $[a(T_n, \rho_n) \times 10^9]$ (m^2 s^{-1})	Heat capacity $C_p(T_n, \rho_n)$ (J mol^{-1} K^{-1})
102	0.437	0.563	0.01003	613.3	29.0
	0.632	0.855	0.01040	371.7	32.7
	0.773	1.092	0.01074	254.1	38.7
112	0.333	0.376	0.01079	994.4	28.9
	0.475	0.548	0.01098	683.6	29.3
	0.654	0.778	0.01126	493.2	29.3
	0.818	1.005	0.01157	369.8	31.1
	0.995	1.269	0.01197	271.5	34.8
	1.203	1.612	0.01259	195.0	40.0
	1.369	1.924	0.01321	145.5	47.2
122	0.556	0.585	0.01193	691.4	29.5
	0.777	0.842	0.01223	455.3	31.9
	1.020	1.144	0.01263	325.4	33.9
	1.255	1.460	0.01310	241.2	37.2
	1.470	1.774	0.01364	188.6	40.8
	1.665	2.086	0.01422	166.5	40.9
	1.817	2.351	0.01475	121.2	51.7
	2.019	2.744	0.01568	94.8	60.3
	2.154	3.037	0.01648	83.3	65.2
	2.331	3.478	0.01791	66.0	78.0
	2.463	3.865	0.01953	57.3	88.2

Table II
The thermal conductivity, thermal diffusivity, and heat capacity of liquid nitrogen

Nominal temperature T_n (K)	Cell pressure P (MPa)	Nominal density $\rho_n(T_n, P)$ (mol ℓ^{-1})	Thermal conductivity $\lambda_n(T_n, \rho_n)$ (W m^{-1} K^{-1})	Thermal diffusivity $[a(T_n, \rho_n) \times 10^9]$ (m^2 s^{-1})	Heat capacity $C_p(T_n, \rho_n)$ (J mol^{-1} K^{-1})
81	1.328	28.305	0.13842	70.1	69.8
	6.699	28.813	0.14477	78.6	63.9
	13.722	29.384	0.15200	79.8	64.8
	21.411	29.923	0.15906	81.3	65.4
	31.130	30.514	0.16700	98.8	55.4
	41.412	31.058	0.17425	91.0	61.6
	53.515	31.621	0.18187	89.1	64.5
	64.951	32.093	0.18877	104.4	56.3
91	3.367	26.817	0.12236	62.5	73.0
	7.132	27.283	0.12781	69.1	67.8
	12.469	27.850	0.13458	74.6	64.8
	17.589	28.322	0.14043	75.4	65.8
	24.897	28.909	0.14798	79.0	64.8
	32.400	29.435	0.15491	90.0	58.5
	40.584	29.942	0.16179	94.4	57.2
	49.867	30.453	0.16881	95.8	57.9
	59.022	30.905	0.17515	93.4	60.7
	67.584	31.291	0.18051	107.1	53.9
102	1.260	24.238	0.09750	50.9	79.0
	3.055	24.648	0.10127	53.8	76.4
	5.540	25.131	0.10596	61.0	69.2
	8.744	25.657	0.11133	65.0	66.7
	12.309	26.159	0.11666	67.2	66.3
	17.001	26.726	0.12309	74.1	62.2
	21.820	27.232	0.12907	75.0	63.2
	27.554	27.760	0.13568	86.0	56.8
	33.758	28.264	0.14215	89.4	56.2
	41.266	28.804	0.14906	94.5	54.8
	49.079	29.304	0.15578	94.3	56.3
	58.455	29.839	0.16335	100.9	54.3
	67.740	30.314	0.16994	103.7	54.0
122	2.982	18.043	0.06034	22.1	151.5
	3.470	18.785	0.06290	26.4	126.6
	4.018	19.360	0.06487	29.2	114.7
	4.738	19.927	0.06706	32.1	104.9
	5.746	20.534	0.07003	38.8	87.8
	8.152	21.567	0.07597	46.1	76.4
	10.818	22.388	0.08157	51.1	71.3
	14.136	23.176	0.08756	59.2	63.9
	18.380	23.975	0.09420	61.8	63.6
	23.313	24.727	0.10102	67.4	60.6
	29.327	25.485	0.10850	72.5	58.7
	36.588	26.248	0.11664	83.9	53.0
	45.777	27.057	0.12572	86.9	53.5
	55.883	27.808	0.13476	94.8	51.1
	67.477	28.548	0.14416	101.0	50.0

Table III
The thermal conductivity, thermal diffusivity, and heat capacity of supercritical nitrogen.

Nominal temperature T_n (K)	Cell pressure P (MPa)	Nominal density $\rho_n(T_n, P)$ (mol ℓ^{-1})	Thermal conductivity $\lambda_n(T_n, \rho_n)$ (W m^{-1} K^{-1})	Thermal diffusivity $[a(T_n, \rho_n) \times 10^9]$ (m^2 s^{-1})	Heat capacity $C_p(T_n, \rho_n)$ (J mol^{-1} K^{-1})
131	0.643	0.627	0.01286	753.5	27.2
	1.100	1.126	0.01347	394.8	30.3
	1.464	1.565	0.01412	274.6	32.9
	1.646	1.800	0.01448	231.0	34.8
	2.198	2.508	0.01593	147.8	41.3
	2.501	3.127	0.01694	114.0	47.5
	2.758	3.631	0.01813	93.8	53.2
	2.972	4.111	0.01938	79.2	59.5
	3.147	4.561	0.02063	65.3	69.3
	3.325	5.086	0.02229	51.5	85.2
	3.452	5.524	0.02383	42.5	101.5
	3.576	6.019	0.02569	44.4	96.2
	3.670	6.457	0.02738	36.2	117.1
	3.750	6.886	0.02918	30.3	140.0
	3.822	7.336	0.03134	25.2	169.6
	3.883	7.769	0.03365	23.7	182.7
	3.932	8.164	0.03534	21.3	203.1
	3.970	8.515	0.03714	20.4	213.6
	4.009	8.895	0.03914	20.1	218.9
	4.046	9.293	0.04066	21.4	204.8
	4.076	9.643	0.04188	21.0	207.3
	4.105	9.986	0.04257	15.5	275.5
	4.157	10.635	0.04392	11.4	363.4
	4.194	11.083	0.04576	10.8	382.6
	4.249	11.731	0.04680	10.8	368.3
	4.300	12.285	0.04728	11.0	348.5
	4.346	12.723	0.04773	11.5	326.1
	4.439	13.463	0.04843	12.7	284.1
	4.511	13.914	0.04890	14.1	249.3
	4.549	14.126	0.04911	14.2	245.1
	4.722	14.883	0.05095	16.9	202.8
	4.931	15.537	0.05210	19.4	172.9
	5.148	16.059	0.05320	23.7	140.0
	5.498	16.706	0.05466	26.7	122.4
	5.763	17.100	0.05572	27.4	118.8
	6.605	18.047	0.05888	33.3	97.9
	7.933	19.066	0.06302	38.7	85.5
	9.441	19.895	0.06680	43.4	77.3
	11.153	20.617	0.07088	47.6	72.2
	13.312	21.338	0.07559	52.9	66.9
	15.936	22.044	0.08034	58.0	62.8
	19.775	22.875	0.08651	67.0	56.5
	24.304	23.664	0.09294	72.9	53.9
	29.017	24.347	0.09900	76.8	52.9
	35.651	25.152	0.10669	80.9	52.4
	43.244	25.924	0.11466	89.5	49.4

Table III (cont.).

Nominal temperature T_n (K)	Cell pressure P (MPa)	Nominal density $\rho_n(T_n, P)$ (mol ℓ^{-1})	Thermal conductivity $\lambda_n(T_n, \rho_n)$ (W m^{-1} K^{-1})	Thermal diffusivity $[a(T_n, \rho_n) \times 10^9]$ (m^2 s^{-1})	Heat capacity $C_p(T_n, \rho_n)$ (J mol^{-1} K^{-1})
	51.985	26.678	0.12290	91.7	50.3
	61.551	27.388	0.13142	99.8	48.1
	68.753	27.863	0.13732	103.9	47.4
152	0.713	0.588	0.01469	906.6	27.6
	1.126	0.952	0.01510	546.2	29.0
	1.753	1.544	0.01581	317.7	32.2
	2.240	2.040	0.01653	233.8	34.6
	2.679	2.521	0.01734	174.7	39.4
	3.137	3.059	0.01824	144.2	41.4
	3.517	3.539	0.01909	119.4	45.2
	3.805	3.925	0.01983	103.9	48.6
	4.191	4.475	0.02094	89.0	52.6
	4.436	4.846	0.02174	80.6	55.7
	4.794	5.421	0.02299	70.4	60.3
	5.103	5.948	0.02420	62.4	65.2
	5.345	6.383	0.02522	69.6	56.8
	5.599	6.857	0.02636	61.7	62.3
	5.793	7.230	0.02729	55.3	68.3
	6.056	7.752	0.02853	52.4	70.3
	6.297	8.241	0.02977	48.9	73.8
	6.510	8.678	0.03091	44.2	80.5
	6.751	9.174	0.03212	41.8	83.7
	6.980	9.643	0.03333	41.7	82.8
	7.185	10.056	0.03443	39.6	86.5
	7.423	10.524	0.03561	38.5	87.8
	7.690	11.030	0.03689	37.9	88.3
	7.916	11.441	0.03801	36.0	92.3
	8.261	12.032	0.03948	36.6	89.7
	8.534	12.470	0.04060	36.8	88.6
	8.919	13.038	0.04212	38.4	84.2
	9.249	13.484	0.04334	38.1	84.4
	9.657	13.989	0.04471	38.7	82.6
	10.191	14.579	0.04643	39.0	81.7
	10.710	15.087	0.04798	40.2	79.1
	11.061	15.401	0.04906	39.7	80.2
	11.989	16.133	0.05155	40.9	78.2
	12.875	16.729	0.05374	42.8	75.1
	13.521	17.115	0.05523	42.2	76.5
	15.010	17.883	0.05850	50.1	65.3
	16.502	18.529	0.06146	53.0	62.5
	18.619	19.296	0.06526	54.7	61.8
	21.561	20.166	0.07010	59.0	58.9
	25.084	21.012	0.07533	66.7	53.8
	28.454	21.689	0.07991	70.5	52.3
	33.226	22.496	0.08589	74.6	51.2
	39.063	23.321	0.09264	78.0	51.0

Table III (cont.).

Nominal temperature T_n (K)	Cell pressure P (MPa)	Nominal density $\rho_n(T_n, P)$ (mol ℓ^{-1})	Thermal conductivity $\lambda_n(T_n, \rho_n)$ (W m^{-1} K^{-1})	Thermal diffusivity $[a(T_n, \rho_n) \times 10^9]$ (m^2 s^{-1})	Heat capacity $C_p(T_n, \rho_n)$ (J mol^{-1} K^{-1})
	45.221	24.058	0.09915	80.7	51.1
	52.326	24.789	0.10615	82.4	51.9
	60.879	25.548	0.11392	98.4	45.3
	69.306	26.201	0.12093	101.4	45.5
177	0.747	0.521	0.01688	1321.0	24.5
	1.326	0.943	0.01733	666.1	27.6
	2.066	1.508	0.01800	401.5	29.7
	2.694	2.012	0.01867	295.9	31.4
	3.201	2.435	0.01928	239.7	33.0
	4.110	3.232	0.02048	176.3	36.0
	4.893	3.959	0.02175	142.3	38.6
	5.588	4.635	0.02292	135.6	36.5
	6.319	5.374	0.02428	115.7	39.1
	7.028	6.112	0.02574	96.2	43.8
	7.700	6.825	0.02723	85.7	46.6
	8.324	7.491	0.02870	78.8	48.7
	9.115	8.331	0.03053	72.0	50.9
	9.841	9.085	0.03224	69.1	51.4
	10.510	9.756	0.03389	65.4	53.1
	11.378	10.584	0.03600	57.6	59.0
	11.991	11.136	0.03739	64.4	52.1
	13.026	12.002	0.03974	58.1	57.0
	13.950	12.705	0.04170	56.9	57.7
	15.004	13.433	0.04374	56.6	57.6
	16.266	14.211	0.04616	56.9	57.0
	17.695	14.987	0.04869	54.8	59.3
	19.209	15.708	0.05133	57.9	56.4
	20.894	16.413	0.05393	58.6	56.1
	23.224	17.254	0.05739	61.3	54.3
	25.412	17.935	0.06058	62.7	53.9
	28.341	18.723	0.06438	67.0	51.3
	32.083	19.577	0.06886	69.6	50.5
	35.562	20.258	0.07289	73.7	48.9
	40.401	21.075	0.07812	76.9	48.2
	45.625	21.830	0.08344	79.8	47.9
	51.754	22.596	0.08911	78.8	50.1
	58.899	23.368	0.09549	82.5	49.6
	67.851	24.202	0.10327	87.7	48.7
203	1.619	0.991	0.01972	669.0	29.7
	2.299	1.426	0.02023	464.2	30.6
	2.985	1.876	0.02081	346.8	32.0
	3.656	2.328	0.02144	286.2	32.2
	4.399	2.839	0.02221	237.1	33.0
	5.371	3.524	0.02325	187.3	35.2
	6.262	4.167	0.02427	157.1	37.1

Table III (cont.).

Nominal temperature T_n (K)	Cell pressure P (MPa)	Nominal density $\rho_n(T_n, P)$ (mol ℓ^{-1})	Thermal conductivity $\lambda_n(T_n, \rho_n)$ (W m^{-1} K^{-1})	Thermal diffusivity $[a(T_n, \rho_n) \times 10^9]$ (m^2 s^{-1})	Heat capacity $C_p(T_n, \rho_n)$ (J mol^{-1} K^{-1})
	6.819	4.574	0.02501	146.5	37.3
	7.543	5.109	0.02596	131.6	38.6
	8.032	5.471	0.02668	124.8	39.1
	8.852	6.080	0.02785	114.7	39.9
	9.493	6.555	0.02889	109.0	40.4
	10.207	7.079	0.02991	102.3	41.3
	10.945	7.614	0.03104	95.7	42.6
	11.584	8.070	0.03204	91.2	43.5
	12.259	8.541	0.03304	87.5	44.2
	13.124	9.128	0.03435	83.8	44.9
	13.977	9.687	0.03576	81.4	45.4
	14.886	10.257	0.03722	79.7	45.5
	16.070	10.960	0.03886	75.9	46.7
	16.817	11.380	0.04002	74.9	47.0
	17.996	12.009	0.04160	72.5	47.8
	19.048	12.534	0.04316	71.5	48.2
	20.331	13.132	0.04484	70.4	48.5
	21.472	13.628	0.04635	70.1	48.5
	22.817	14.171	0.04813	70.3	48.3
	24.236	14.703	0.04984	69.9	48.5
	25.761	15.230	0.05184	70.7	48.1
	27.147	15.675	0.05329	69.2	49.1
	28.903	16.196	0.05538	71.2	48.1
	31.014	16.770	0.05772	71.6	48.1
	32.943	17.250	0.05988	73.0	47.5
	35.021	17.727	0.06213	73.5	47.7
	37.769	18.303	0.06497	75.1	47.3
	40.746	18.868	0.06794	76.9	46.8
	42.924	19.249	0.07002	78.7	46.2
	45.990	19.746	0.07285	78.8	46.8
	49.727	20.298	0.07626	80.9	46.5
	53.714	20.834	0.07977	83.7	45.7
	58.345	21.400	0.08367	84.8	46.1
	63.152	21.933	0.08758	87.6	45.6
	67.958	22.422	0.09141	90.0	45.3
228	0.977	0.521	0.02135	1513.9	27.0
	2.084	1.127	0.02193	676.0	28.8
	2.538	1.379	0.02215	524.4	30.6
	3.529	1.938	0.02280	360.9	32.6
	4.181	2.311	0.02345	322.4	31.5
	4.957	2.759	0.02406	270.9	32.2
	5.976	3.354	0.02498	223.2	33.4
	6.894	3.894	0.02571	186.4	35.4
	7.776	4.415	0.02660	169.2	35.6
	8.883	5.068	0.02774	150.4	36.4
	9.857	5.641	0.02878	136.8	37.3

Table III (cont.).

Nominal temperature T_n (K)	Cell pressure P (MPa)	Nominal density $\rho_n(T_n, P)$ (mol ℓ^{-1})	Thermal conductivity $\lambda_n(T_n, \rho_n)$ (W m^{-1} K^{-1})	Thermal diffusivity $[a(T_n, \rho_n) \times 10^9]$ (m^2 s^{-1})	Heat capacity $C_p(T_n, \rho_n)$ (J mol^{-1} K^{-1})
	10.597	6.072	0.02948	125.5	38.7
	11.491	6.586	0.03044	116.2	39.8
	12.538	7.178	0.03157	107.5	40.9
	13.445	7.679	0.03254	100.8	42.0
	14.394	8.191	0.03362	97.0	42.3
	15.415	8.726	0.03491	95.4	42.0
	16.425	9.236	0.03611	92.2	42.4
	17.567	9.792	0.03736	88.4	43.2
	18.752	10.343	0.03865	84.8	44.1
	20.010	10.900	0.04003	81.7	44.9
	21.319	11.450	0.04145	80.0	45.2
	22.752	12.018	0.04303	77.8	46.0
	24.306	12.597	0.04465	77.6	45.7
	25.817	13.124	0.04645	79.6	44.5
	27.653	13.723	0.04828	77.6	45.3
	29.261	14.211	0.04996	77.9	45.1
	31.259	14.777	0.05180	77.4	45.3
	32.751	15.172	0.05327	78.7	44.6
	34.972	15.723	0.05547	78.8	44.8
	37.622	16.327	0.05787	78.6	45.1
	39.799	16.785	0.05974	77.9	45.7
	43.255	17.452	0.06279	79.5	45.2
	46.406	18.006	0.06561	81.7	44.6
	49.655	18.531	0.06821	81.3	45.2
	52.813	19.002	0.07062	81.8	45.4
	55.981	19.442	0.07359	87.1	43.5
	59.673	19.918	0.07620	87.1	43.9
	63.915	20.424	0.07956	89.3	43.6
	68.849	20.965	0.08337	92.0	43.2
253	1.963	0.946	0.02356	824.7	30.2
	3.034	1.471	0.02424	552.2	29.8
	4.126	2.012	0.02485	397.5	31.1
	5.065	2.479	0.02552	325.1	31.7
	6.401	3.147	0.02649	262.5	32.1
	7.783	3.839	0.02756	220.6	32.5
	8.858	4.374	0.02836	186.7	34.7
	10.085	4.980	0.02944	167.6	35.3
	11.170	5.510	0.03038	155.1	35.5
	12.584	6.188	0.03166	140.8	36.3
	14.102	6.898	0.03294	126.6	37.7
	15.785	7.658	0.03443	116.3	38.7
	17.911	8.573	0.03651	108.8	39.1
	19.207	9.104	0.03781	105.5	39.4
	19.208	9.105	0.03779	104.6	39.7
	20.001	9.420	0.03836	105.3	38.7
	21.409	9.960	0.03966	101.3	39.3

Table III (cont.).

Nominal temperature T_n (K)	Cell pressure P (MPa)	Nominal density $\rho_n(T_n, P)$ (mol ℓ^{-1})	Thermal conductivity $\lambda_n(T_n, \rho_n)$ (W m^{-1} K^{-1})	Thermal diffusivity $[a(T_n, \rho_n) \times 10^9]$ (m^2 s^{-1})	Heat capacity $C_p(T_n, \rho_n)$ (J mol^{-1} K^{-1})
	23.048	10.560	0.04105	95.2	40.8
	24.726	11.141	0.04271	95.0	40.4
	26.566	11.742	0.04418	91.5	41.1
	28.595	12.365	0.04600	91.2	40.8
	31.123	13.084	0.04882	97.4	38.3
	32.933	13.565	0.04983	89.0	41.3
	33.587	13.732	0.05006	84.3	43.3
	34.980	14.077	0.05160	87.3	42.0
	36.191	14.365	0.05206	83.9	43.2
	37.382	14.639	0.05338	86.9	42.0
	38.146	14.809	0.05392	87.2	41.7
	39.869	15.180	0.05527	84.7	43.0
	40.588	15.330	0.05612	88.5	41.4
	42.413	15.697	0.05716	83.3	43.7
	42.648	15.743	0.05744	85.2	42.8
	45.457	16.270	0.05942	82.8	44.1
	46.050	16.377	0.06006	86.2	42.5
	48.483	16.799	0.06203	87.0	42.4
	48.617	16.821	0.06200	86.2	42.7
	51.671	17.315	0.06415	86.2	43.0
	51.792	17.334	0.06451	87.3	42.6
	54.395	17.728	0.06615	86.1	43.3
	55.896	17.945	0.06728	86.2	43.5
	58.190	18.265	0.06886	88.3	42.7
	60.181	18.530	0.07046	87.4	43.5
	61.640	18.718	0.07121	87.6	43.4
	64.302	19.049	0.07302	85.8	44.7
	65.372	19.177	0.07373	87.3	44.1
	68.382	19.526	0.07634	91.3	42.8
	68.739	19.566	0.07659	93.0	42.1
278	1.145	0.497	0.02496	2040.9	24.6
	2.318	1.011	0.02547	935.8	26.9
	3.555	1.555	0.02596	586.4	28.5
	4.480	1.962	0.02648	467.7	28.9
	6.134	2.691	0.02744	351.9	29.0
	7.787	3.415	0.02855	278.8	30.0
	9.680	4.236	0.02988	226.7	31.1
	11.363	4.953	0.03091	186.6	33.4
	13.155	5.700	0.03217	163.5	34.5
	14.873	6.396	0.03347	151.8	34.5
	16.844	7.165	0.03499	138.1	35.4
	18.910	7.940	0.03648	127.4	36.1
	20.720	8.587	0.03798	120.1	36.8
	23.138	9.406	0.03974	113.4	37.3
	25.528	10.166	0.04158	107.5	38.0
	27.906	10.874	0.04337	100.7	39.6

Table III (cont.).

Nominal temperature T_n (K)	Cell pressure P (MPa)	Nominal density $\rho_n(T_n, P)$ (mol ℓ^{-1})	Thermal conductivity $\lambda_n(T_n, \rho_n)$ (W m^{-1} K^{-1})	Thermal diffusivity $[a(T_n, \rho_n) \times 10^9]$ (m^2 s^{-1})	Heat capacity $C_p(T_n, \rho_n)$ (J mol^{-1} K^{-1})
	30.775	11.670	0.04548	96.2	40.5
	33.341	12.331	0.04749	95.7	40.2
	36.685	13.128	0.04984	95.6	39.7
	40.116	13.877	0.05228	101.7	37.0
	43.755	14.605	0.05488	99.4	37.8
	47.761	15.337	0.05744	92.6	40.4
	52.708	16.156	0.06076	92.9	40.5
	57.357	16.853	0.06395	91.0	41.7
	62.398	17.541	0.06722	92.2	41.6
	71.104	18.595	0.07278	100.9	38.8
303	1.326	0.527	0.02670	1896.2	26.7
	2.560	1.019	0.02717	926.3	28.8
	3.849	1.532	0.02767	596.1	30.3
	4.977	1.980	0.02826	471.2	30.3
	6.186	2.458	0.02872	348.8	33.5
	7.892	3.127	0.02988	296.9	32.2
	10.025	3.951	0.03097	237.4	33.0
	11.913	4.665	0.03197	205.4	33.4
	13.959	5.419	0.03324	177.0	34.6
	16.210	6.221	0.03451	153.6	36.1
	18.229	6.914	0.03599	148.4	35.1
	20.555	7.678	0.03751	135.5	36.1
	22.952	8.428	0.03891	120.5	38.3
	25.429	9.161	0.04055	119.9	36.9
	28.104	9.908	0.04236	114.3	37.4
	30.771	10.607	0.04420	110.1	37.8
	33.834	11.358	0.04619	106.0	38.4
	37.308	12.147	0.04821	105.3	37.7
	40.902	12.902	0.05067	102.3	38.4
	44.751	13.647	0.05316	99.4	39.2
	48.754	14.360	0.05545	103.0	37.5
	53.596	15.150	0.05845	99.6	38.7
	58.410	15.866	0.06137	108.2	35.7
	63.617	16.576	0.06423	100.4	38.6
	70.762	17.454	0.06859	91.2	43.1

densities. If the critical enhancement is appreciable, a curvature in the temperature rise plots is found, probably because of compressibility effects not yet accounted for. Under these circumstances the error increases from low densities to the critical density and decreases above the critical density. The error attributed to each data point can be characterized by the linear regression uncertainties generated during the fitting of lines to the temperature rise as a function of log of time. Statistics for both the slope and intercept are recorded

in ref. [24]. A better measure of the data uncertainty is provided by the dispersion of the results at different powers. This is also provided in ref. [24]. Considering the variation in applied powers, the uncertainty in thermal conductivity is ±0.6% for the lowest densities along an isotherm and decreases to ±0.2% for liquid densities. If there is an appreciable critical enhancement, the uncertainty, considering the variation in applied powers, increases near the critical density up to about ±3% for the 130 K isotherm, which is the nearest to the critical temperature. Fig. 2 displays the variation of the thermal conductivi-

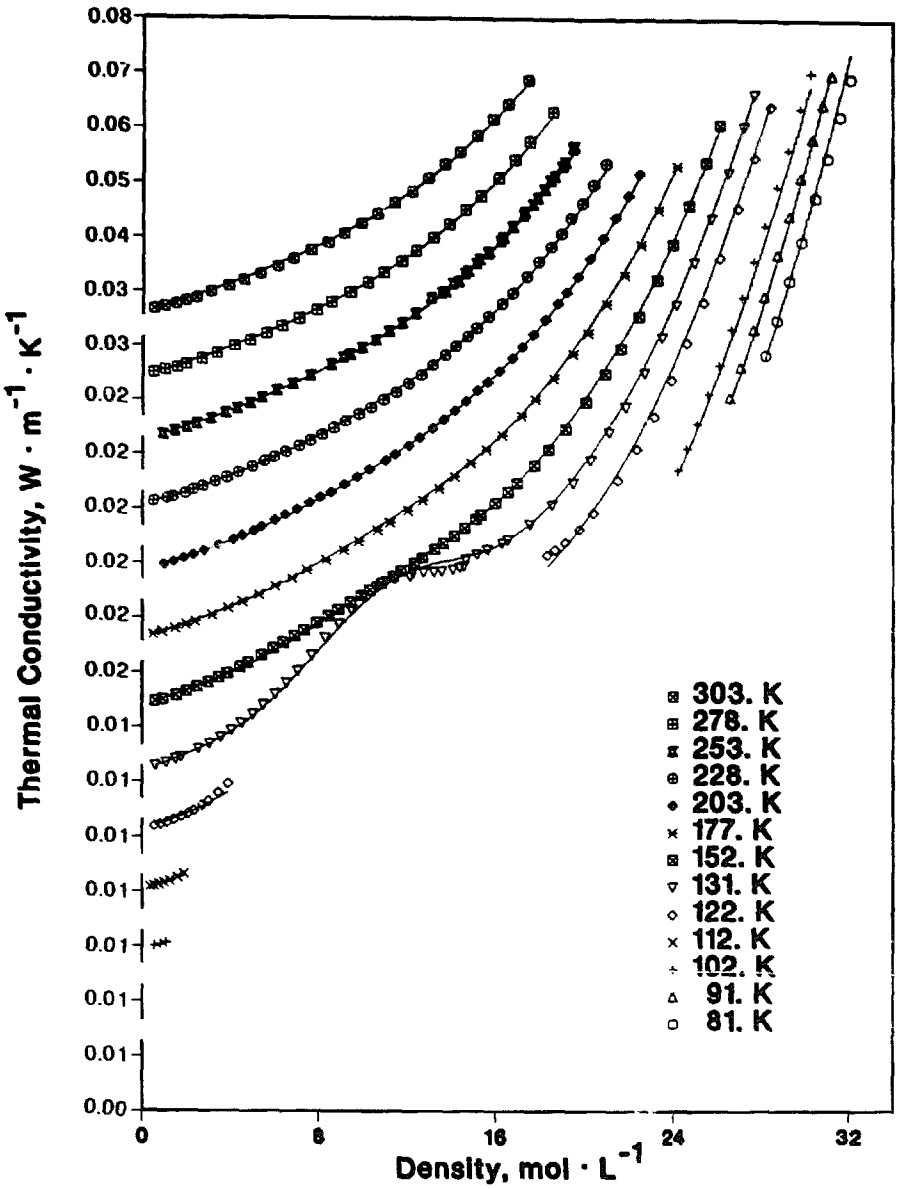

Fig. 2. The thermal conductivity of nitrogen along with the values calculated from the reported surface fit. Isotherms are seperated by 0.010 W m^{-1} K^{-1} to show details.

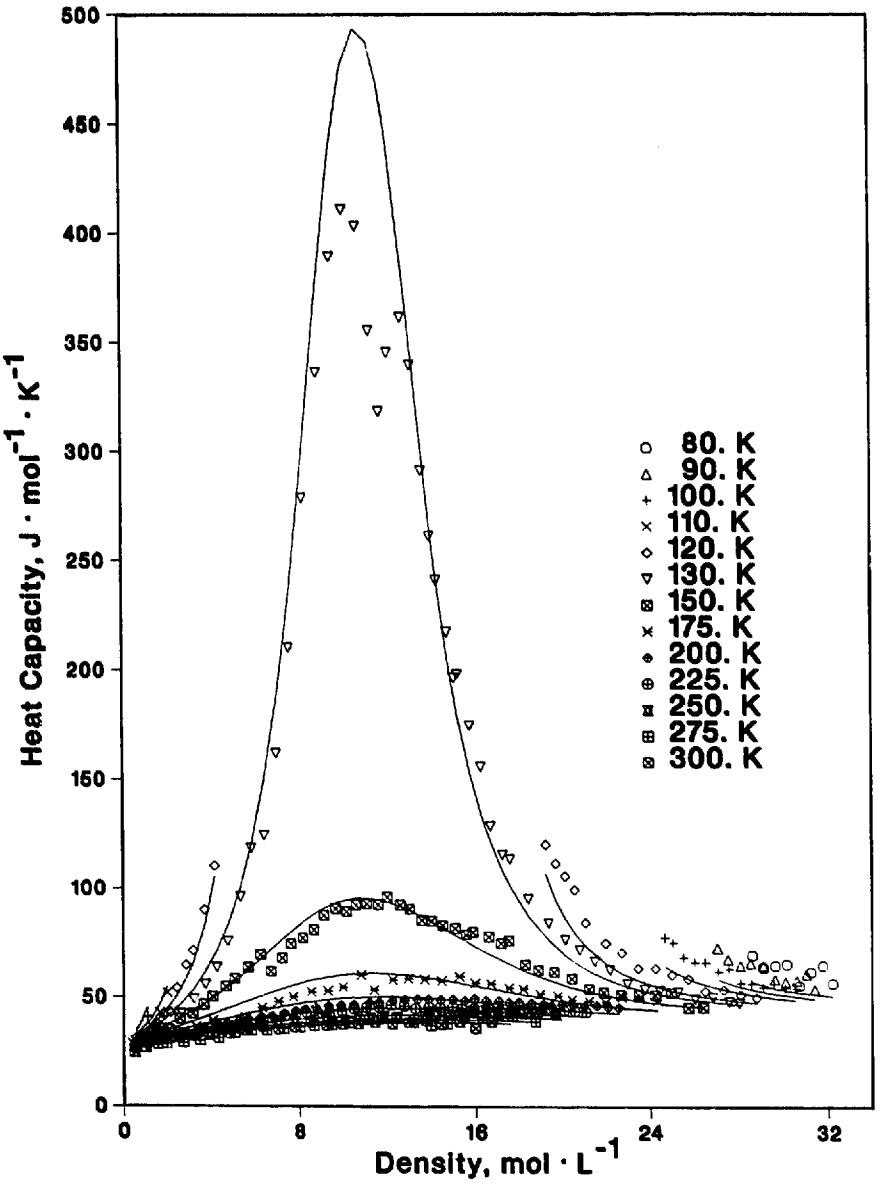

Fig. 3. The isobaric heat capacity of nitrogen along with values from the equation of state of Jacobsen et al. [27].

ty with density for the different isotherms. The lines in fig. 2 correspond to the values calculated from the surface fit described in this paper.

The values of the measured thermal diffusivity have been adjusted to the nominal temperature and are displayed in tables I, II and III. Errors in the thermal diffusivity exhibit a pattern similar to that of the thermal conductivity. Considering the variation in applied powers, the uncertainty in the thermal diffusivity is ±5% for densities above 1 mol ℓ^{-1} and decreases to ±3% for liquid densities. If there is an appreciable critical enhancement, the error

increases. For example, the uncertainty in thermal diffusivity is about ±10% for the 130 K isotherm at the critical density.

The heat capacity was obtained from the values of thermal diffusivity, and thermal conductivity adjusted to the cell temperature and pressure, and the density from the equation of state of Jacobsen et al. [27]. The tables also show the values of the heat capacity adjusted to the nominal temperatures using the equation of state. Fig. 3 shows the experimental heat capacities along with lines representing the corresponding values calculated from the equation of state [27]. The root-mean-square deviation between the experimental data and the values obtained from the equation of state [27] is about 5%. The equation of state [27] appears to be systematically lower than our data in the high pressure, compressed liquid region. This is probably due to a lack of liquid phase isobaric heat capacity data during the development of the equation of state. Jacobsen et al. [27] indicate that no liquid phase isobaric heat capacity data were available at pressures above 13 MPa.

5. Data analysis

The results presented in tables I, II and III represent a major addition to the nitrogen thermal conductivity data available below 300 K. The thermal conductivity can be written as the sum of three terms according to

$$\lambda = \lambda_0(T) + \Delta\lambda_{\text{excess}}(\rho, T) + \Delta\lambda_{\text{crit}}(\rho, T)\,. \tag{4}$$

The first term is the dilute gas term and is a function of temperature only. The second is the excess thermal conductivity, which is generally a function of temperature and density. The final term is the critical enhancement, which is a function of temperature and density.

5.1. *Dilute gas thermal conductivity*

The low density thermal conductivity can be expanded in a density power series of the form

$$\lambda = \lambda_0(T) + \lambda_1(T)\,\rho + \ldots, \tag{5}$$

where $\lambda_0(T)$ is the dilute gas thermal conductivity and $\lambda_1(T)$ is the first density coefficient of thermal conductivity. It is generally possible to represent the thermal conductivity of nitrogen up to the phase boundary or to about 3 mol ℓ^{-1} as a linear function of density, and to obtain both $\lambda_0(T)$ and $\lambda_1(T)$.

The isotherms are highly curved near the critical temperature, even for densities below 3 mol ℓ^{-1}. On these isotherms, the maximum density considered is reduced until an acceptable linear fit is obtained. The values obtained from linear isothermal fits of the data are presented in table IV.

The zero density thermal conductivity is obtained from a linear extrapolation of the low density data for each isotherm. Table IV shows the values obtained for $\lambda_0(T)$ and for the initial slope with respect to density $\lambda_1(T)$, along with their standard deviations, for the vapor and supercritical gas. Table IV also shows the maximum density of the data points used in the linear fit.

The λ_0 values can be adequately represented by a second order polynomial in temperature. This functional form of λ_0 was used along with the functional forms below for $\Delta\lambda_{\text{excess}}$ and $\Delta\lambda_{\text{crit}}$ in a nonlinear regression of all of our data. Thus the coefficients reported in this section and the following two sections are the result of this nonlinear regression. In the equation for dilute gas thermal conductivity,

$$\lambda_0(T) = A_1 + A_2 T + A_3 T^2 , \tag{6}$$

the optimized coefficients are given by

$$A_1 = -1.57480 \times 10^{-3} , \qquad A_2 = 1.14388 \times 10^{-4} ,$$
$$A_3 = -7.65412 \times 10^{-8} ,$$

where λ_0 is in W m^{-1} K^{-1} and T is in K.

Table IV
The dilute gas thermal conductivity and the first density coefficient of nitrogen as a function of temperature.

T (K)	λ_0 (mW m^{-1} K^{-1})	Std. dev.	λ_1 (mW m^{-1} K^{-1} ℓ mol^{-1})	Std. dev.	$\rho_{(\max)}$ (mol ℓ^{-1})
102.0	9.27	0.08	1.33	0.09	1.09
112.0	10.26	0.04	1.32	0.05	1.27
122.0	11.14	0.05	1.33	0.04	1.46
131.0	12.00	0.06	1.33	0.05	1.56
152.0	13.92	0.10	1.26	0.08	2.04
177.0	16.18	0.06	1.25	0.04	2.43
203.0	18.33	0.07	1.35	0.04	2.84
228.0	20.58	0.16	1.22	0.09	2.76
253.0	22.38	0.13	1.26	0.07	2.48
278.0	24.33	0.10	1.12	0.06	2.69
303.0	26.10	0.17	1.07	0.11	2.46

5.2. Excess thermal conductivity

The form initially selected for the excess thermal conductivity is a polynomial in density. The general expression we use is

$$\Delta\lambda_{\text{excess}}(\rho, T) = \alpha(T)\,\rho + \beta(T)\,\rho^2 + \gamma(T)\,\rho^3 + \delta(T)\,\rho^4\,, \tag{7}$$

where α, β, γ and δ are linear functions of temperature. During the surface fit of the nitrogen data we found that the excess function is very nearly temperature independent. This conclusion is in agreement with results of several other researchers [3, 13] for nitrogen. The resulting expression for the thermal conductivity excess function is therefore simplified to

$$\Delta\lambda_{\text{excess}}(\rho, T) = B_1\rho + B_2\rho^2 + B_3\rho^3 + B_4\rho^4\,, \tag{8}$$

where the optimized coefficients are

$$B_1 = 1.18325 \times 10^{-3}\,, \qquad B_2 = 2.90297 \times 10^{-5}\,,$$
$$B_3 = 8.53486 \times 10^{-7}\,, \qquad B_4 = 8.50205 \times 10^{-8}\,,$$

with $\Delta\lambda_{\text{excess}}$ in $\mathrm{W\,m^{-1}\,K^{-1}}$, ρ in $\mathrm{mol\,\ell^{-1}}$, and T in K.

5.3. Critical enhancement

The combination of the dilute gas thermal conductivity and the excess thermal conductivity is often termed the background thermal conductivity in the context of critical enhancement studies. The experimental critical enhancement is obtained by subtracting the background thermal conductivity from the experimental data. We follow our previous analysis [18, 28] and select a function of the form $\exp(-x^2)$ to represent the critical enhancement. The variable x is a simple function of density chosen to be 0 at the maximum value of the critical enhancement. The nitrogen data do not seem to exhibit a significant asymmetry about the critical density, as reported for some other fluids [18, 28]. As a result, we center the critical enhancement about the critical density 11.177 $\mathrm{mol\,\ell^{-1}}$ [27], and the variable x is of the form $x = \gamma(\rho - \rho_c)$. The maximum value of $\Delta\lambda_{\text{crit}}$ is the amplitude (AMPL) of the function for the particular temperature under consideration. The amplitude is chosen to be a simple function of temperature with 4 parameters. The complete expression for the critical enhancement becomes

$$\Delta\lambda_{\text{crit}}(\rho, T) = \text{AMPL}\,\mathrm{e}^{-x^2}\,, \tag{9}$$

where

$$\mathrm{AMPL} = C_1(T' + C_2)^{-1} + C_3 + C_4 T' \tag{10}$$

and

$$x = C_5(\rho - \rho_c)\,. \tag{11}$$

For temperatures above the critical point, $T' = T$. For temperatures below the critical point we define $T' = 2T_c - T$. The parameter C_5 reflects the width of the critical enhancement and appears to be constant for the nitrogen data. The optimized coefficients are

$$C_1 = 8.35308 \times 10^{-2}\,, \qquad C_2 = -1.25000 \times 10^{2}\,, \qquad C_3 = 2.23744 \times 10^{-3}\,,$$
$$C_4 = -8.23063 \times 10^{-6}\,, \qquad C_5 = 2.0798 \times 10^{-1}\,,$$

with $\Delta\lambda_{\mathrm{crit}}$ in $\mathrm{W\,m^{-1}\,K^{-1}}$, ρ in $\mathrm{mol\,\ell^{-1}}$, and T in K. None of our data fall into the asymptotically critical region, so the density can be obtained with a classical equation of state.

6. Discussion

The discusson can be divided into four parts. First, we compare the data obtained in the zero density limit with data and correlations previously reported [19–21]. Second, we compare our experimental first density thermal conductivity coefficients with the predictions of the kinetic theory of Rainwater and Friend [29, 30]. Third, we compare our experimental critical enhancement with the mode coupling theory recently proposed by Olchowy and Sengers [42]. Finally, the thermal conductivity data surface is compared with other data and correlations available in the literature.

6.1. Low density limit

The thermal conductivity data and the resulting surface fit which have been described can be compared with existing experimental data, the Younglove correlation [19, 31], and the correlation proposed by Stephan et al. [20]. Fig. 4 shows a deviation plot of such a comparison and also includes the recent low density correlation of Millat and Wakeham [21]. The literature data [3, 4, 7, 8, 11–13, 15] are generally from 0.5 to 2% higher than our results. We suspect that these differences are due to differences in the application of the various

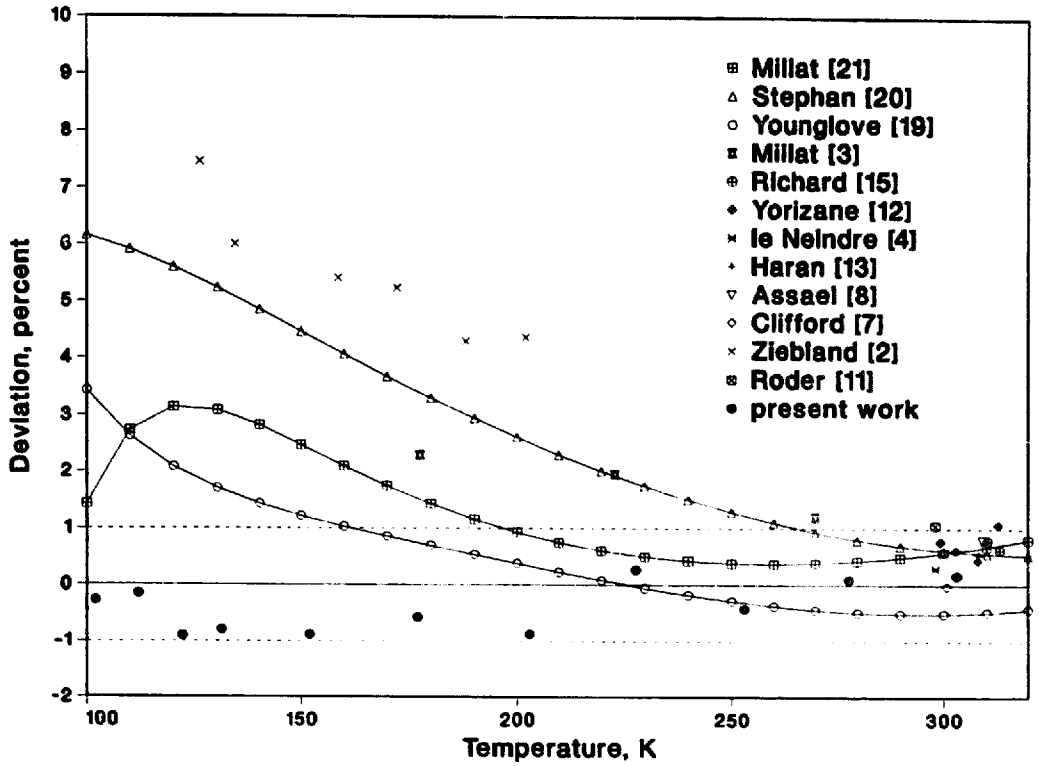

Fig. 4. Deviation plot of the dilute gas thermal conductivity relative to our reported polynomial fit. Deviations between the correlations of Millat and Wakeham [21], Stephan et al. [20] and Younglove [19] are also shown.

transient hot wire temperature corrections. For instance, not using the black-body thermal radiation correction, which is often assumed to be negligible, results in a 1% increase in the measured thermal conductivity for nitrogen at 300 K. Our results near 303 K agree with measurements made with this instrument in 1981 [11] within 0.5%. The older low temperature data obtained by Ziebland and Burton [2] deviate considerably from both our data and the low temperature data of Millat et al. [3].

The correlations of Millat and Wakeham [21] and Younglove [19] both agree well with the present data although they are both higher than our data by 0.75 to 3%. The deviations are largest at the lower temperatures where reliable data were not previously available. Our data agree well with the correlation of Millat and Wakeham [21] down to 100 K even though the lower temperature limit proposed by these authors is 120 K. The correlation of Stephan et al. [20] has deviations up to 6% at low temperatures. Stephan et al. [20] used only 2 data points below 300 K in the development of their correlation. Although the stated range of the correlation of Stephan et al. [20] is 70 K to 1100 K, the correlation was evidently quite speculative at temperatures below 300 K.

6.2. First density coefficient

There have been several attempts to theoretically predict the first density coefficient of thermal conductivity. Two of them are variants of the original work of Enskog [32, 33], which adapt the kinetic theory of a dense hard sphere fluid to real systems. These schemes, called modified Enskog theory (MET), were discussed by Hanley et al. [34], and by Kestin, Mason and coworkers [35, 36]. The modified Enskog theories cannot accurately predict λ_1 [25, 37].

Following a different route, several authors attempted to formulate a theory for the first density coefficient of a monatomic gas, which is based on the Lennard-Jones 12–6 potential [29, 30, 37–39]. All these authors have identified a number of different contributions to the first density coefficient of thermal conductivity including collisonal transfer and three-body interactions.

The most recent and comprehensive treatment has been given by Rainwater and Friend [29, 30], and we shall restrict our comparisons to their model, which includes two-monomer, three-monomer, and monomer–dimer contributions and which was originally developed for monatomic systems. They define a reduced thermal conductivity virial coefficient B_λ^* by

$$B_\lambda^* = \frac{3B_\lambda}{2\pi N_A \sigma^3}\,, \tag{12}$$

where $B_\lambda = \lambda_1/\lambda_0$ (see eq. (5)), N_A is Avogadro's number, and σ is the Lennard-Jones molecular diameter. The reduced thermal conductivity virial coefficient is a universal function of reduced temperature for a given interaction potential. The reduced temperature ($T^* = k_B T/\epsilon$) is defined in terms of the Lennard-Jones energy parameter ϵ and the Boltzmann constant k_B.

Following the approach of Millat et al. [3], we use the MET to define a reduced first density coefficient for polyatomic molecules such that the internal degrees of freedom are accounted for. For polyatomic gases, such as nitrogen, the reduced first density coefficient is defined as

$$B_\lambda^* = \frac{3B_\lambda \lambda_0}{2\pi N_A \sigma^3 \lambda_{0,\mathrm{tr}}} + 0.625\left[\left(\frac{\lambda_0}{\lambda_{0,\mathrm{tr}}}\right) - 1\right], \tag{13}$$

with

$$\lambda_{0,\mathrm{tr}} = \frac{15R\eta_0}{4M} \tag{14}$$

equal to the translational contribution to the dilute gas thermal conductivity. In these equations, η_0 is the dilute gas viscosity taken from the dilute gas correlation of Stephan et al. [20], M is the molecular mass, R is the universal

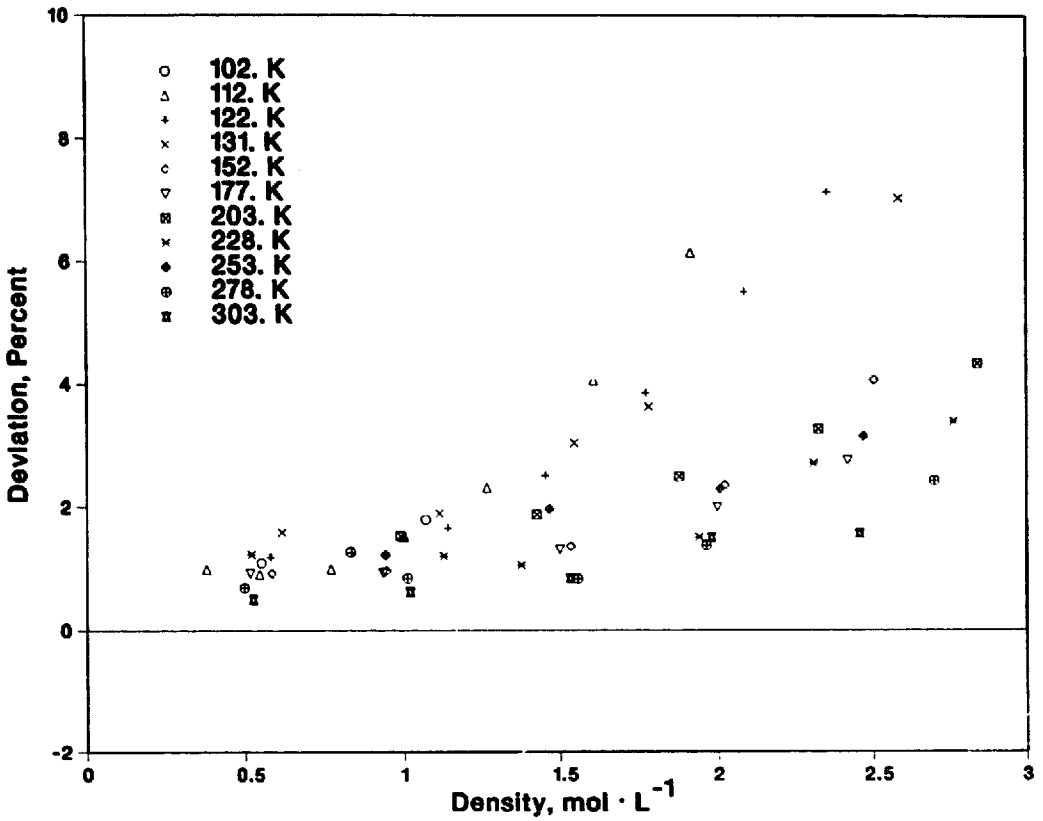

Fig. 5. Deviation plot of moderately dense gaseous nitrogen relative to the theory of Rainwater and Friend [29, 30]. Theoretical values are given by $\lambda = \lambda_0(1 + B_\lambda \rho)$, where λ_0 is the experimental isotherm extrapolation and B_λ is the predicted thermal conductivity virial coefficient.

gas constant, λ_0 is taken as the experimental dilute gas thermal conductivity, and B_λ is from the theoretical calculations [29, 30].

Fig. 5 shows the deviations between the experimental data presented in this paper and the values predicted by the theory using ... (13) and (14). The deviations are generally within 2% over the range of 0 to 2 mol ℓ^{-1}. Substantial curvature is seen for the subcritical vapor isotherms ($T = 102$, 112 and 122 K) and for the near critical supercritical isotherms ($T = 131$ and 152 K). Most of this curvature is due to critical enhancement contributions to the thermal conductivity. Comparisons between the experimental and theoretical B_λ for several monatomic and polyatomic gases, including nitrogen, have recently been reported [40]. The present nitrogen results are systematically higher than the theoretical predictions, but are in agreement with the experimental results of Haran et al. [13].

6.3. *Critical enhancement*

A theory describing the divergence of the thermal conductivity in the asymptotically critical region has been well developed for pure fluids [41].

More recently, Olchowy and Sengers have proposed a solution to the mode-coupling equations which allows calculation of the thermal conductivity enhancement throughout the fluid state [42]; a simplified version of this theory, which incorporates an ad hoc procedure and approximates the full theory, has also been published [43]. The theory has been used successfully to describe transport data of carbon dioxide, methane, ethane, helium 3 and water [42–46].

The approach involves the approximate solution of coupled integral equations with a wave number cutoff (q_D) to limit the momentum–space range over which critically driven fluctuations can contribute to dynamic critical phenomena. Thus, in addition to knowledge of thermodynamic properties and background values of the viscosity and thermal conductivity, the single fluid-dependent parameter q_D must be fitted to describe the critical enhancement contribution. In this work, we have used the classical nitrogen equation of state and critical parameters of Jacobsen et al. [27], the fluid-dependent equilibrium critical amplitudes of Sengers et al. [41], and the scaling law exponents of Olchowy and Sengers [42]. We have also used the viscosity correlation of Stephan et al. [20]. Because none of our data are in the asymptotically critical region, we do not need a scaling-law equation of state, and the viscosity, which has a much weaker critical enhancement than the thermal conductivity [47], can be well approximated by its background contribution.

The thermal conductivity enhancement can be described by [42]

$$\Delta\lambda_{\text{crit}} = \frac{R_c k_B T \rho C_p}{6\pi\eta\xi} (\Omega - \Omega_0) , \tag{15}$$

where the amplitude R_c has been set to 1.01, k_B is the Boltzmann constant, ξ is the correlation length, and Ω and Ω_0 are complicated functions of T and ρ briefly described below.

The correlation length ξ has been approximated by relating it to the critical part of the dimensionless compressibility as in refs. [42–46]. Thus we write

$$\xi = \xi_0 \left[\frac{P_c \rho}{\Gamma \rho_c^2}\right]^{\nu/\gamma} \left[\left.\frac{\partial\rho(\rho, T)}{\partial P}\right|_T - \left(\frac{T_r}{T}\right) \left.\frac{\partial\rho(\rho, T_r)}{\partial P}\right|_T\right]^{\nu/\gamma} . \tag{16}$$

The temperature at which the background compressibility has been identified with the total compressibility, so that the critical contribution vanishes, is not well defined. This temperature T_r is well above the critical temperature and has variously been defined as $1.5T_c$, approximately $2T_c$, and $2T_c$ in refs. [42–46]. Because our nitrogen data clearly indicate an enhancement (although small) when studying various deviation plots for isotherms above $2T_c$ (252.386 K), we

have increased the value of T_r to $2.5T_c$. The correlation length for critical fluctuations, and hence the critical enhancement, vanishes above this temperature; and both ξ in eq. (16) and $\Delta\lambda_{crit}$ in eq. (15) should be set to 0 for temperatures above $2.5T_c$. The choice of T_r is arbitrary, and affects the calculated enhancement only at temperatures well above the critical temperature.

The function Ω in eq. (15) can be evaluated using the parameters

$$y_D = q_D\xi\,, \tag{17a}$$

$$y_\gamma = C_V/(C_p - C_V)\,, \tag{17b}$$

$$y_\alpha = k_B TM\rho/8\pi\eta^2\xi\,, \tag{17c}$$

$$y_\beta = (\lambda_0 + \Delta\lambda_{excess})M/\eta(C_p - C_V)\,, \tag{17d}$$

and

$$y_\delta = \{\tan^{-1}[q_D\xi/(1+q_D^2\xi^2)^{1/2}] - \tan^{-1}(q_D\xi)\}/(1+q_D^2\xi^2)^{1/2}\,, \tag{17e}$$

where C_V is the isochoric heat capacity and the other variables have been defined above. We have simplified the final expression for Ω from refs. [42, 43, 45], by evaluating the mode-coupling integral in closed algebraic form; the matrix inversion algorithm required to use the results reported by Sengers and Olchowy [42, 44, 45], is no longer necessary. We can write

$$\Omega = \frac{2}{\pi(1+y_\gamma)}\left[y_D + \sum_{i=1}^{4}\left(\frac{g(z_i)\,(1-z_i^2)^{-1/2}}{\prod_{i\neq j=1}^{4}(z_i - z_j)} \times \ln\left(\frac{1 - z_i + (1-z_i^2)^{1/2}\tan^{-1}(\frac{1}{2}y_D)}{1 - z_i - (1-z_i^2)^{1/2}\tan^{-1}(\frac{1}{2}y_D)} \right) \right) \right]. \tag{18}$$

The auxiliary function $g(z)$ is defined by

$$g(z) = -y_D y_\alpha z^3 + (y_\gamma - y_\beta - y_\alpha y_\delta)z^2 - y_\gamma y_D y_\alpha z + y_\gamma^2 - y_\gamma y_\delta y_\alpha\,, \tag{19}$$

and z_i are the roots of the quartic equation

$$\prod_{i=1}^{4}(z - z_i) = z^4 + y_\alpha y_D z^3 + (y_\gamma + y_\beta + y_\delta y_\alpha)z^2 + y_\alpha y_D y_\gamma z + y_\alpha y_\delta y_\gamma = 0\,. \tag{20}$$

The roots can be found in closed algebraic form by standard procedures such as that described in section 3.8.3 of the handbook of Abramowitz and Stegun [48]; in that case, the first 2 roots are typically real and the final 2 roots are complex conjugates. The expression in eq. (18) is real, although the arguments may be complex. Our definition of the z_i differs by a minus sign from that published in refs. [42–46].

The final term Ω_0 in eq. (15) represents the contribution of dynamical fluctuations to the thermal conductivity, which is caused by the long-time tail of their correlations [42–46, 49]. This term must be subtracted in eq. (15) so that the experimental thermal conductivity well away from the critical region can be identified with the background thermal conductivity; these contributions are thus included in the background correlation rather than in the enhancement term described by eq. (15). We have retained the empirical term proposed by Olchowy and Sengers [42–46], but have slightly revised the denominator appearing in Ω_0. The term Ω_0 is defined by

$$\Omega_0 = \frac{2\left[1 - \exp\left(\dfrac{-q_D\xi}{1 + q_D^3\xi^3\rho_c^2/3\rho^2}\right)\right]}{\pi[1 + y_\alpha y_D + y_\beta/(1 + y_\gamma)]} . \tag{21}$$

The term Ω_0 rigorously cancels Ω to lowest order in an expansion about $q_D\xi = 0$, that is, well away from the critical point. We have removed from the denominator of Ω_0 the term which does not explicitly contribute to the term cancellation; other higher-order terms remain in the exponential and the denominator. Our revision of Ω_0 has only a small effect on the enhancement calculated from eq. (15) since its contribution is important only to points far from the critical point where the total enhancement is negligible.

We chose values for the universal and fluid-dependent parameters as indicated above: $R_c = 1.01$, $\nu = 0.63$, $\gamma = 1.2415$, $T_c = 126.193$ K, $\rho_c = 11.177$ mol ℓ^{-1}, $\Gamma = 0.075$, and $\xi_0 = 0.16$ nm. We computed the experimental value of the thermal conductivity critical enhancement by subtracting the background term, as determined by the sum of the correlation equations (6) and (8), from the experimental total thermal conductivity. Many of these values of the experimental critical enhancement are very small, often of the order of 0.1 mW m^{-1} K^{-1}, since the range of experimental temperatures and pressures is so large; some values are negative since the background is imperfectly determined and the experimental thermal conductivities have accuracies of the order of 1%. Thus in determining the single parameter q_D, we emphasized the data near the 131, 152 and 177 K isotherms, especially in the range from 0.5 to 1.5 times ρ_c. We obtained $q_D^{-1} = 0.213$ nm, and fig. 6 illustrates the theoretical enhancement obtained from eq. (15).

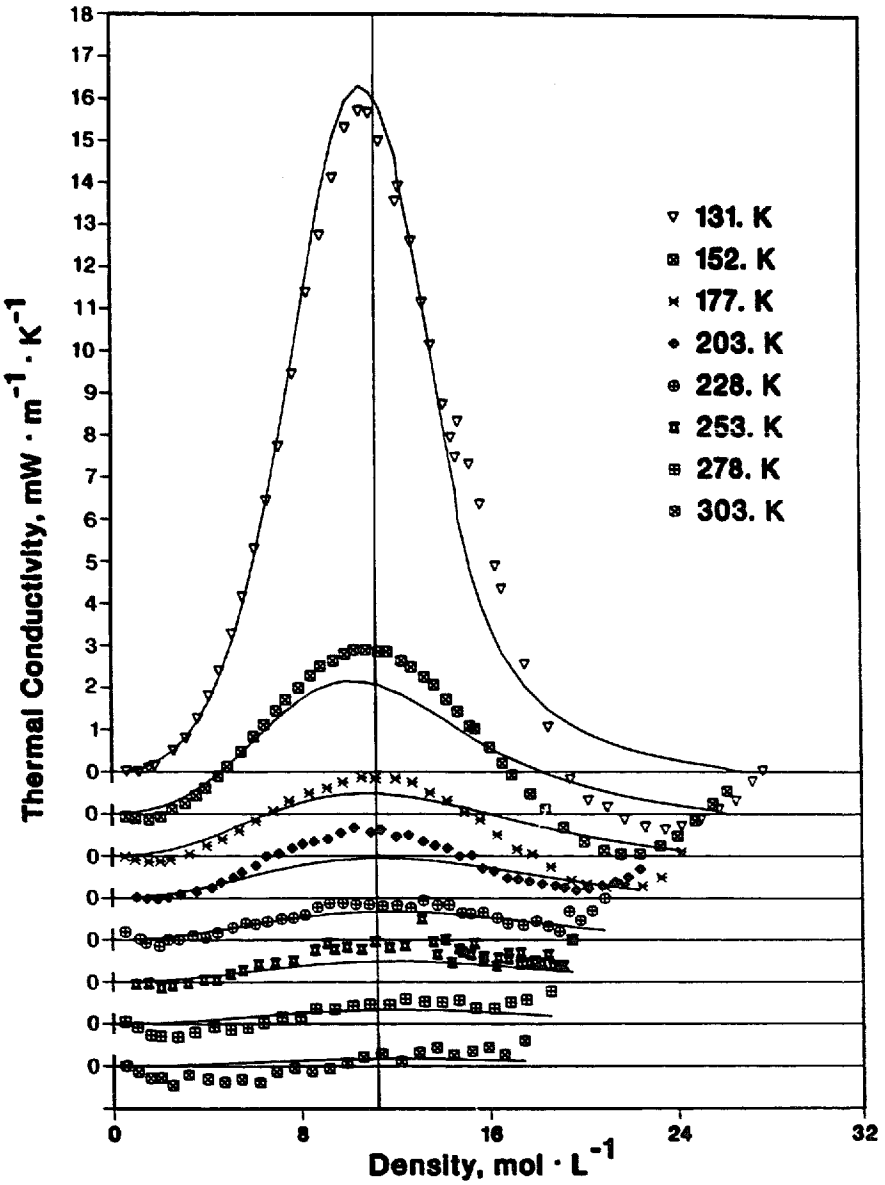

Fig. 6. The thermal conductivity critical enhancement for nitrogen. The background thermal conductivity has been obtained from our surface fit. Lines are calculated with the mode coupling theory of Olchowy and Sengers [42].

The agreement between the theoretically based curves and the data, which have been adjusted to lie along true isotherms using the global correlation of eqs. (6)–(10), is good. We emphasize that the mode-coupling theory of Olchowy and Sengers was not used during the surface fit. Thus it is not surprising that some systematic differences are seen between the data and the curves, especially at densities with intermediate supercritical or subcritical values. An adjustment of the background, or multiple iterations between the background fitting and determinations of q_D, could be used to minimize these

systematic discrepancies. The quality of the fit of the enhancement is not greatly sensitive to small adjustments in q_D. The average absolute deviation of the enhancement calculated from eq. (15), compared to the 1511 values of the measured thermal conductivity enhancement, is 0.51 mW m^{-1} K^{-1}; a value of 0.46 mW m^{-1} K^{-1} is obtained when the enhancement is calculated from eq. (9). We take the agreement between the critical enhancement from our surface fit and that obtained from the mode-coupling theory of Olchowy and Sengers as an indication that we have a good representation of the thermal conductivity excess function.

6.4. *Data surface*

Fig. 7 shows the deviations between our correlation, eqs. (6)–(11), and other data and correlations near 300 K. The maximum deviation between our surface fit and our data on this isotherm is 1.5%. Nitrogen has been studied previously with an early version of our instrument [11], and the agreement with the present data is within the claimed accuracy of both data sets, although the present data are up to 1% lower at elevated pressures. Good agreement, within their combined uncertainties, is also found between the present data and

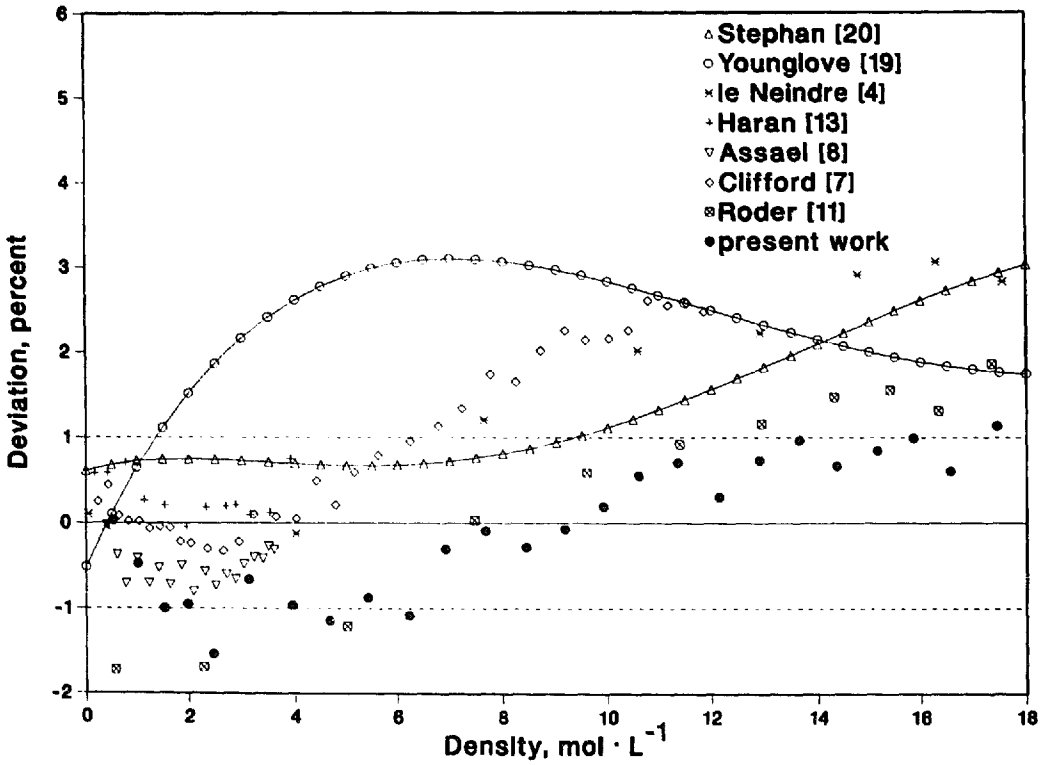

Fig. 7. Deviation plot of nitrogen thermal conductivity near 300 K relative to our surface fit. Deviations from the correlations of Younglove [19] and Stephan et al. [20] are also shown. Data have been adjusted to 300 K using our surface correlation.

the steady-state concentric cylinder data of le Neindre [4]. The transient hot wire data of several researchers [7, 8, 13] appear to be systematically larger than our data by up to 2%, although the claimed accuracy of these data sets is less than 0.5%. This discrepancy has also been noted by Stephan et al. [20] in the development of their thermal conductivity excess function. The excess function of Stephan et al. [20] agrees well with all of the available data. Near 300 K the excess function of Younglove [19] deviates substantially from the available data.

A complete summary of the deviations between our thermal conductivity data and various correlations over the entire surface is provided in table V. Our thermal conductivity surface generally fits the data within ±1%, with the largest deviations occurring on the compressed liquid isotherms. Our correlation is limited to the region from 80 to 300 K at pressures to 70 MPa. Although the Younglove [19] correlation does very well for the prediction of λ_0, it exhibits significant deviations at other densities as shown in fig. 7. The Younglove correlation [19] has average deviations from 2–6% in the supercritical region and predicts too much critical enhancement on the 131 K near-critical isotherm. The Younglove correlation also underpredicts the subcritical vapor phase thermal conductivity.

Table V
Comparison of the percentage average absolute deviation (AAD) and the percentage BIAS for the present correlation, the Younglove correlation [19], and the correlation of Stephan et al. [20].

Isotherm temperature (K)	AAD present work	BIAS present work	AAD ref. [19]	BIAS ref. [19]	AAD ref. [20]	BIAS ref. [20]
Vapor						
102.000	0.232	−0.206	7.200	−7.200	2.420	2.420
112.00	1.280	0.727	6.821	−6.821	2.880	2.880
122.000	0.538	−0.442	6.597	−2.822	2.710	2.710
Liquid						
81.000	1.287	−1.287	3.596	−3.596	2.367	2.367
91.000	0.969	−0.901	6.032	−0.241	2.834	2.834
102.000	2.277	−1.088	6.999	6.999	4.388	0.384
122.000	1.578	0.602	2.310	1.738	4.471	4.133
Supercritical						
131.000	1.413	0.465	5.898	5.754	13.400	−9.953
152.000	0.799	−0.111	5.866	5.833	4.645	−0.914
177.000	0.694	0.636	3.206	3.206	2.900	1.701
203.000	0.386	−0.262	1.967	1.962	2.072	1.007
228.000	0.446	0.028	2.113	2.103	1.448	1.263
253.000	0.577	−0.385	1.540	1.492	1.458	1.136
278.000	0.504	0.127	2.051	2.046	1.185	1.177
303.000	0.713	0.354	2.370	2.361	1.420	1.420

The correlation of Stephan et al. [20] generally does better in the liquid and vapor regions where the average deviation is typically between 2–3%. The thermal conductivity excess function of Stephan et al. [20] is in good agreement with our data. Errors in the λ_0 function of Stephan et al. [20] contribute significantly to these average deviations at temperatures below 250 K. Additional errors are encountered in the critical region due to the fact that the correlation of Stephan et al. [20] made no provision for the critical enhancement contribution, which becomes significant at temperatures between 126 and 200 K.

7. Conclusions

Extensive new measurements of the thermal conductivity of nitrogen have been reported; they have an uncertainty less than ±1% except near the critical point. Thermal diffusivities and isobaric heat capacities are also reported, which have an estimated uncertainty of ±5%. These thermal diffusivities also provide an internal consistency check of our thermal conductivity data. Near the critical point, the uncertainty in the thermal conductivity and thermal diffusivity increases to ±3% and ±10%, respectively. The thermal conductivity measurements are consistent with our previous measurements of nitrogen [11]. These results are generally 1 to 2% lower than the transient hot wire measurements of several other researchers [3, 7, 8, 13–15]. A surface fit of our data is provided which provides a good representation of our data.

The experimental λ_0 values are in good agreement with the correlations of Millat and Wakeham [21] and Younglove [19]. The first density coefficient values are in good agreement with the thermal conductivity virial theory of Rainwater and Friend [30]. The thermal conductivity excess function is found to be very nearly temperature independent over a very wide range of temperatures for nitrogen. The thermal conductivity critical enhancement which we obtain experimentally, is in good agreement with the crossover theory of Olchowy and Sengers [42] and extends to nearly 2.5 times the critical temperature.

The fact that the thermal conductivity critical enhancement extends over a wide range of temperature severely complicates the study of the thermal conductivity excess function. Even if the excess function is only a function of density, as we have found for nitrogen, it may also appear to be a function of temperature if the critical enhancement is not properly accounted for. For instance, on the lowest temperature isotherm of Millat et al. [3] at 177.5 K, our results indicate that the critical enhancement reached a maximum of 1.5 mW m^{-1} K^{-1} at 8 mol ℓ^{-1}. This amounts to a critical enhancement contribu-

tion of 4.8% at the highest pressure measured on this isotherm. Yet, since the maximum density studied never exceeded the critical density, these authors apparently did not realize that there was a significant critical enhancement on this isotherm. This could easily be misinterpreted as temperature dependence in the excess function.

We conclude that it is necessary to study a fluid over a wide range of temperatures and densities in order to characterize the thermal conductivity surface. It is not sufficient to characterize $\lambda_0(T)$ along with the thermal conductivity excess function at high reduced temperatures in order to describe the thermal conductivity surface. The critical enhancement must be considered at temperatures up to 2.5 times the critical temperature given the accuracy and speed of modern transient hot wire thermal conductivity instruments.

Acknowledgements

We thank Arno Laesecke for many helpful discussions regarding the development of his wide range correlation of nitrogen transport properties and the magnitude of errors associated with assuming a temperature independent thermal conductivity excess function. D.G. Friend gratefully acknowledges financial support from the United States Department of Energy, Division of Chemical Sciences, Office of Basic Energy Sciences.

References

[1] A. Uhlir, J. Chem. Phys. 20 (1952) 463.
[2] H. Ziebland and J.T.A. Burton, Br. J. Appl. Phys. 9 (1958) 52.
[3] J. Millat, M.J. Ross and W.A. Wakeham, Physica A 159 (1989) 28.
[4] B. le Neindre, Int. J. Heat Mass Transfer 15 (1972) 1.
[5] F.G. Keyes and R.G. Vines, J. Heat Transfer 87 (1965) 177.
[6] D. Misic and G. Thodos, AIChE J. 11 (1965) 650.
[7] A.A. Clifford, J. Kestin and W.A. Wakeham, Physica A 97 (1979) 287.
[8] M.J. Assael and W.A. Wakeham, J. Chem. Soc. Faraday Trans. I 77 (1981) 697.
[9] X.Y. Zheng, S. Yamamoto, H. Yoshida, H. Masuoka and M. Yorizane, J. Chem. Eng. Jpn. 17 (1984) 237.
[10] R. Tufeu and B. le Neindre, Int. J. Thermophys. 1 (1980) 375.
[11] H.M. Roder, J. Res. Nat. Bur. Stand. 86 (1981) 457.
[12] M. Yorizane, S. Yoshimura, H. Masuoka and H. Yoshida, Industr. Eng. Chem. Fund. 22 (1983) 454.
[13] E.N. Haran, G.C. Maitland, M. Mustafa and W.A. Wakeham, Ber. Bunsenges. Phys. Chem. 87 (1983) 657.
[14] A.A. Clifford, P. Gray, A.I. Johns, A.C. Scott and J.T.R. Watson, J. Chem. Soc. Faraday Trans. I 77 (1981) 2679.
[15] R.G. Richard and I.R. Shankland, Int. J. Thermophys. 10 (1989) 673.

[16] H.M. Roder and C.A. Nieto de Castro, in: Thermal Conductivity, vol. 20, D.P.H. Hasselman and J.R. Thomas, eds. (Plenum, New York, 1988) p. 173.
[17] C.A. Nieto de Castro, B. Taxis, H.M. Roder and W.A. Wakeham, Int. J. Thermophys. 9 (1988) 293.
[18] H.M. Roder, R.A. Perkins and C.A. Nieto de Castro, Int. J. Thermophys. 10 (1989) 1141.
[19] B.A. Younglove, J. Phys. Chem. Ref. Data 11, Suppl. 1 (1982).
[20] K. Stephan, R. Krauss and A. Laesecke, J. Phys. Chem. Ref. Data 16 (1987) 993.
[21] J. Millat and W.A. Wakeham, J. Phys. Chem. Ref. Data 18 (1989) 565.
[22] C.A. Nieto de Castro, Jpn. Soc. Mech. Eng. Int. J. Series II 31 (1988) 387.
[23] H.M. Roder and C.A. Nieto de Castro, Cryogenics 27 (1987) 312.
[24] H.M. Roder, R.A. Perkins and C.A. Nieto de Castro, Nat. Inst. Stand. Tech. (U.S.) Interagency Rept. 88–3902, Oct. (1988).
[25] J.M.N.A. Fareleira and C.A. Nieto de Castro, High Temp. High Pressure 21 (1989) 363.
[26] U.V. Mardolcar, C.A. Nieto de Castro and W.A. Wakeham, Int. J. Thermophys. 7 (1986) 259.
[27] R.T. Jacobsen, R.B. Stewart and M. Jahangiri, J. Phys. Chem. Ref. Data 15 (1986) 735.
[28] H.M. Roder, Int. J. Thermophys. 6 (1985) 119.
[29] D.G. Friend and J.C. Rainwater, Chem. Phys. Lett. 107 (1984) 590.
[30] J.C. Rainwater and D.G. Friend, Phys. Rev. A 36 (1987) 4062.
[31] H.J.M. Hanley and J.F. Ely, J. Phys. Chem. Ref. Data 2 (1973) 735.
[32] J.H. Ferziger and H.G. Kaper, Mathematical Theory of Transport Processes in Gases (North-Holland, Amsterdam, 1972).
[33] J.O. Hirschfelder, C.F. Curtiss and R.B. Bird, The Molecular Theory of Gases and Liquids (Wiley, New York, 1954).
[34] H.J.M. Hanley, R.D. McCarty and E.D.G. Cohen, Physica 60 (1972) 322.
[35] R. DiPippo, J.R. Dorfman, J. Kestin, H.E. Khalifa and E.A. Mason, Physica A 86 (1977) 205.
[36] E.A. Mason, H.E. Khalifa, J. Kestin, R. DiPippo and J.R. Dorfman, Physica A 91 (1978) 377.
[37] S.K. Kim and J. Ross, J. Chem. Phys. 42 (1965) 263.
[38] D.K. Hoffman and C.F. Curtiss, Phys. Fluids 8 (1965) 890.
[39] R.D. Olmsted and C.F. Curtiss, J. Chem. Phys. 63 (1975) 1966.
[40] C.A. Nieto de Castro, D.G. Friend, R.A. Perkins and J.C. Rainwater, Chem. Phys. 145 (1990) 19.
[41] J.V. Sengers, R.S. Basu and J.M.H. Levelt Sengers, NASA Contractor Report 3424 (1981).
[42] G.A. Olchowy and J.V. Sengers, Phys. Rev. Lett. 61 (1988) 15.
[43] G.A. Olchowy and J.V. Sengers, Int. J. Thermophys. 10 (1989) 417.
[44] G.A. Olchowy and J.V. Sengers, Representative Equations for the Transport Properties of Carbon Dioxide in the Critical Region, University of Maryland Technical Report BN 1052, College Park, MD (1986).
[45] G.A. Olchowy, Crossover from Singular to Regular Behavior of the Transport Properties of Fluids in the Critical Region, Ph.D. Thesis, University of Maryland, College Park, MD (1989).
[46] R. Mostert, H.R. van den Berg, P.S. van der Gulik and J.V. Sengers, J. Chem. Phys. 92 (1990) 5454.
[47] V.N. Zozulya and Y.P. Blagoi, Sov. Phys. JETP 3 (1974) 99.
[48] M. Abramowitz and I.A. Stegun, Handbook of Mathematical Functions, Appl. Math. Series 55 (1964); reprinted by: (Dover, New York, 1972).
[49] J.R. Dorfman and E.G.D. Cohen, Phys. Rev. A 6 (1972) 776.